View Article Online
DOI: 10.1039/C6CC08229G

ChemComm

COMMUNICATION

On the efficacy of anthracene isomers for triplet transmission from CdSe nanocrystals†

Received 00th January 20xx,
Accepted 00th January 20xx

DOI: 10.1039/x0xx00000x

www.rsc.org/

Pan Xia,[a] Zhiyuan Huang,[b] Xin Li,[b] Juan J. Romero,[cd] Valentine I. Vullev,[bc] George Shu Heng Pau,[e] Ming Lee Tang*[ab]

The effect of isomeric substitutions on the transmitter for triplet energy transfer (TET) between nanocrystal (NC) donor and molecular acceptor is investigated. Each isomeric acceptor is expected to bind in a unique orientation with respect to the NC donor. We see that this orbital overlap drastically affects the transmission of triplets. Here, two functional groups, the carboxylic acid and dithiocarbamate, were varied between the 1-, 2- and 9- positions of the anthracene ring to give three ACA and three ADTC isomers. These six anthracene isomers served as transmitters for triplets between CdSe NC sensitizers and 9, 10-diphenylanthracene annihilators for photon upconversion. The photon upconversion quantum yield (QY) is the highest for 9-ACA (12%), lowest for 9-ADTC (0.1%), around 3% for both 1-ACA and 1-ADTC, and about 1 % for the 2-isomers. These trends in QYs are reflected in the rates of TET given by ultrafast transient absorption spectroscopy where a maximum of 3.8 x10^7 s^{-1} for 9-ACA was measured. Molecular excited state energy levels were measured both in solution and polymer hosts to correlate structure to TET. This work confirms that anthracene excited states levels are very sensitive to molecular substitution, which in combination with orbital overlap, critically affect Dexter-based TET.

Hybrid materials made of organic and inorganic components may deliver synergies in charge or energy transfer. This is seen in perovskite and dye-sensitized solar cells (DSSCs). Perovskite solar cells have an inherently long charge carrier diffusion lengths,[2,3] resulting in an unrivalled trajectory in their power conversion efficiencies,[4,5] especially when compared to other thin-film alternatives. DSSCs combine mesoporous titania with bound organo-metallic compounds to efficiently convert photons into current.[6-8] In terms of energy transfer, semiconductor nanocrystals (NCs), in conjunction with acene derivatives, have been demonstrated to upconvert light incident at solar fluxes effectively.[9-14] In all these hybrid systems, an atomic and molecular understanding of the organic-inorganic interface is critical in enhancing electronic communication between the various components. Investigation of the mechanism and factors affecting energy conversion are key to designing efficient solar light harvesting and converting structures. In fact, for the DSSCs, it has been shown that the conjugated backbone, functional group, metal center, etc. the dye can drastically affect electron transfer to the titania photoanode.[15-18]

With this in mind, it is clear that similar considerations must apply to all hybrid platforms. Here, the focus is on a hybrid photon upconversion system, specifically on how molecular orientation and orbital overlap affects triplet energy transfer (TET) from NC donor to anthracene transmitter. We investigate the electronic communication between different isomers of anthracene transmitter ligands covalently bound to CdSe NCs, especially because excited states are very sensitive to environmental factors and molecular substitutions in anthracene.[19-21] Electronic communication is evaluated with two independent and complementary methods, transient absorption (TA) measurements and continuous wave (cw) photon upconversion experiments. This was motivated by our earlier observation that the 1-, 2- and 9- anthracene carboxylic acid (**ACA**) transmitter ligands gave noticeably different upconversion QYs for the conversion of green to violet light[9]. Using TA spectroscopy, we find that **9-ACA** transmits triplets at rates two orders of magnitude higher than **1-** and **2- ACA**, giving the highest upconversion QY of 12%, while the 9-anthracene dithiocarbamate (**9-ADTC**) quenches the CdSe 100x faster than the **1-** and **2-ADTC** with a low upconversion QY of 0.1%. The 9-isomers effect energy or charge transfer at rates on the order of 10^7 s^{-1}, while the 2-isomers and 1-isomers have upconverison QYs of 1 % and 3% respectively with rates of TET around 10^5 s^{-1}. We hypothesize that the low upconversion QY for **9-ADTC** may be due to the intramolecular charge transfer states which are reflected in the inherently low fluorescence QY of these dithiocarbamate (**DTC)** containing ligands.

Six different anthracene transmitter ligands were used in this study. They consist of anthracene substituted with either carboxylic acid or dithiocarbamate at the 1-, 2- or 9- positions of the conjugated ring (Fig. 1a). These functional groups bind

[a] *Materials Science & Engineering Program, University of California, Riverside, Riverside, CA 92521.*
[b] *Department of Chemistry, University of California, Riverside, Riverside, CA 92521,USA. E-mail: mltang@ucr.edu*
[c] *Department of Bioengineering, University of California, Riverside, Riverside, CA 92521, USA.*
[d] *Present address: Instituto de Investigaciones Fisicoquímicas Teóricas y Aplicadas (INIFTA), Facultad de Ciencias Exactas, Universidad Nacional de La Plata, Casilla de Correo 16, Sucursal 4, (1900) La Plata, Argentina.*
[e] *Earth Sciences Division, Lawrence Berkeley National Laboratory, Berkeley, CA 94720, USA.*
†Electronic Supplementary Information (ESI) available: See DOI: 10.1039/x0xx00000x

View Article Online
DOI: 10.1039/C6CC08229G

the anthracene moiety onto the surface of 2.39 nm diameter(half width at half maximum of the first exciton absorption is 14 nm)

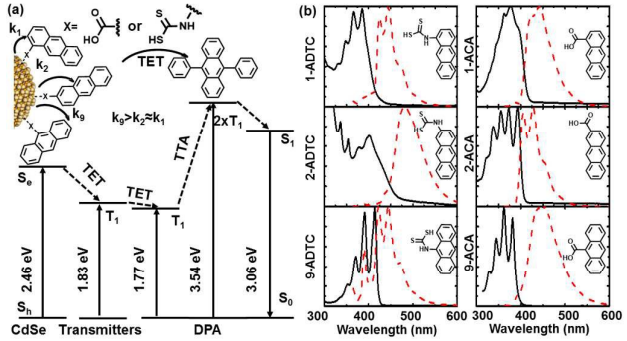

Fig. 1 (a) Schematic of the energy transfer in this hybrid photon upconversion system, with 2.39 nm diameter CdSe nanocrystals (NCs) as sensitizer and **DPA** as annihilator. Isomeric anthracene derivatives functionalized with carboxylic acid and dithiocarbamate binding groups at the 1-, 2- and 9- positions on the aromatic ring serve as transmitter ligands with different rates of triplet energy transfer for each isomer (k_1, k_2 and k_9 respectively). (b) Emission (dash line) and absorption (solid line) spectra of **1-ACA**, **2-ACA**, **9-ACA**, **1-ADTC**, **2-ADTC** and **9-ADTC** ligands in tetrahydrofuran at RT.

wurtzite octadecylphosphonic acid (**ODPA**) functionalized CdSeNCs (CdSe/**ODPA**). In this hybrid organic-inorganic upconversion system, energy is transferred from the CdSe NCs (sensitizer) to the triplet state of the transmitter down an energy cascade to the 9, 10-diphenylanthracene (**DPA**) annihilator. Two **DPA** molecules in their triplet excited states collide with each other and undergo triplet-triplet annihilation (TTA) to emit a photon higher in energy than the incident light. Fig. 1b shows the electronic absorption and fluorescence spectra of the **ACA** and **ADTC** isomers in anhydrous THF at RT. Details are listed in Table S1. Comparing the emission of **1-ADTC**, **9-ADTC** and **2-ACA**, the red-shifted, broad emission of **2-ADTC**, **1-ACA** and **9-ACA** (λ_{ex} = 350 nm) with little vibrational fine structure is consistent with the functional group being coplanar with the anthracene ring, as described by Werner and Hercules, and later by Ghoneim.[22,23] This bathochromic shift is solvent dependent. While the **ACA** isomers are commercially available, the **ADTC** isomers were synthesized in two steps (see Scheme 1 in the SI). Firstly, 9-nitroanthracene was reduced to 9-aminoanthracene in 72% yield.[24] The **DTC** target molecules were obtained by the nucleophilic attack of the amine isomers on carbon disulfide with ~ 90% yield for all **ADTC** isomers.[25] The **ACA** isomers were chosen to further investigate the high upconversion QY (14%) obtained with the **9-ACA** transmitter.[9] In comparison with the carboxylic acid, the dithiocarbamate functional group was expected to lower the tunnelling barrier for energy transfer across the NC-transmitter interface with the formation of a more covalent bond.[26] However, since the Weiss group showed that phenyl dithiocarbamates delocalize the CdSe excitonic hole onto the ligands,[27] charge transfer states stemming from interaction of the conjugated core with the **DTC** functional group could also inhibit TET across this interface with the formation of a more covalent bond.[26]

The **ADTC** isomers bind more strongly to the **ODPA**-coated CdSe NCs (CdSe/**ADTC**) than their **ACA** counterparts (CdSe/**ACA**). Using UV-Vis electronic absorption spectroscopy, we have shown there are an average of three **9-ACA** transmitter ligands bound per CdSe NC. Fig. S1 shows that the dithiocarbamate group binds more strongly than the carboxylic acid group to the chalcogenide NCs. For the **ADTC** transmitters, 3 to 15 ligands are bound per NC even though the ratio of **ADTC** per NC is lower during ligand exchange. In contrast, for the **ACA** isomers, *N*, the average number of bound transmitter ligands per NC, is 2- 6 even when the transmitter concentration is 10 times higher and ligand exchange time longer, up to 12 hours.

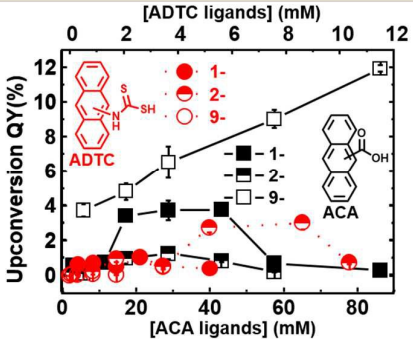

Fig. 2 (a) the relationship between upconversion QY (%) and the transmitter concentration of **ACA** isomers (squares) and **ADTC** (circles) exchange. All upconversion samples were air-free in hexane with **DPA** annihilator concentration of 2.15 mM, excited with 12.7 W/cm^2 532 nm or 488 nm cw lasers at RT.

Transmitter		Upconversion QY(%)	*N*	<τ>/ ns	<k> ×10^7 /s^{-1}
No transmitter		0.025[10]	0	39.9	-
ADTC isomer	1-	3.0±0.4	6	39.7	0.075
	2-	1.1±0.1	2	39.9	0.063
	9-	0.1 ±0.0	1	19.5	2.7
ACA isomer	1-	3.8 ±0.4	3	39.7	0.077
	2-	1.2 ±0.3	2	39.9	0.063
	9-	11.9 ±0.2	4	16.0	3.8

Table 1 Maximum upconversion QY (%) and *N*, the average number of bound **ACA** and **ADTC** transmitter ligands per CdSe NC. <τ>, the average lifetime and <k>, the average rate of energy transfer were obtained from fitting a stretched exponential to the kinetic decays at 505 nm in the transient absorption spectra.

In general, anthracene transmitters functionalized at the 1-position are more effective compared to the 2- position in mediating energy transfer. This can be seen in Table 1 and Fig. 2, where CdSe/**1-ADTC** and CdSe/**1-ACA** complexes give upconversion QYs of ~3%, compared to CdSe/**2-ADTC** and CdSe/**2-ACA** NCs which result in upconversion QYs ~1%. Figure 2 shows that the decrease in the upconversion QY after a certain optimal ligand loading may be due to TTA between surface bound transimtters. Table 1 lists the maximum upconversion QYs for each transmitter ligand and the corresponding surface coverage. Fig. 2 shows the upconversion QY (%) as the concentration of **ACA** and **ADTC** concentration in the ligand exchange solution is varied. CdSe/**9-ACA** NCs shows the highest upconversion QY at around 12%, approximately 10 times higher than CdSe/**2-ACA**, while the CdSe/**9-ADTC** NCs have the lowest upconversion QY at 0.1%. The upconversion QY (%) is defined as

$$\Phi_{UC} = 2 \cdot \Phi_{ref} \cdot \frac{photons\ absorbed\ by\ R}{photons\ absorbed\ by\ S} \cdot \frac{photons\ emitted\ by\ S}{photons\ emitted\ by\ R} \quad \text{(eq. 1)}$$

where R and S are reference and sample respectively. The upconverted emission of **DPA** and photoluminescence of CdSe NCs are shown in Fig. S2. Details of the ligand exchange procedure and characterization, including the average number of bound ligands per NC, *N*, are in the SI.

The appearance of the triplet excited states of anthracene (~433 nm) in the CdSe/ transmitter complexes in ultrafast TA experiments confirm direct TET from CdSe NCs to surface-anchored ligands, as

View Article Online
DOI: 10.1039/C6CC08229G

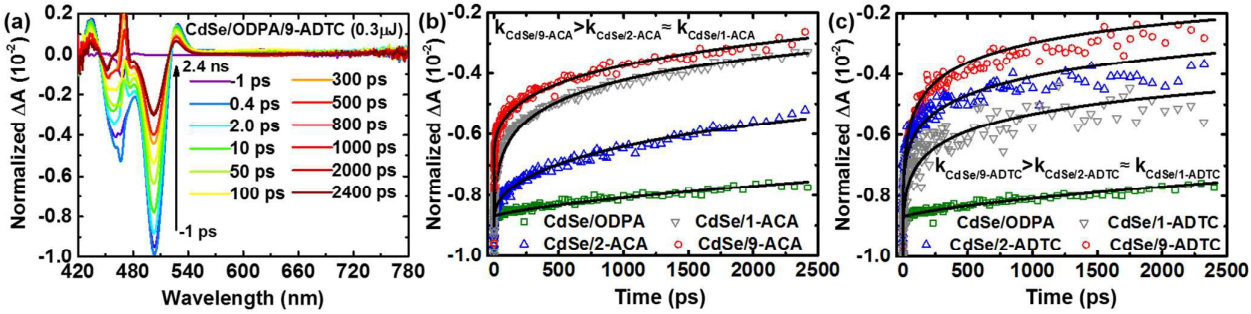

Fig. 3. (a) Ultrafast TA spectra of CdSe/ **9-ADTC** (16.6 μM) using 465 nm pulsed laser excitation (0.3 μJ per pulse, > 30 fs full width at half maximum) in toluene at RT. Experimental decays from 1 picoseconds (ps) before excitation (violet) to 2.4 ns after excitation (red) is shown. (b) and (c) The ground state recovery of CdSe NCs investigated by its kinetics at 505nm, highlighting much faster quenching of its first excitonic state in the presence of transmitter ligands. Native CdSe/**ODPA** (green square) (b) CdSe/**ACA**: **1-ACA** (grey triangle), **2-ACA** (blue triangle) and **9-ACA** (red circle); and (c) CdSe/**ADTC**: **1-ADTC** (grey triangle), **2-ADTC** (blue triangle) and **9-ADTC** (red circle). The black solid line is the fit.

seen in the report by Castellano et al.[13] To aviod multi-exciton annihilation, the pump power was kept at 0.3 μJ (> 30 fs full width at half maximum). TA spectra was acquired for up to 2.4 ns for each optimized CdSe/ transmitter complex with the highest upconversion QY. The decay of the first excited state of CdSe NCs coincided with the growth of an absorption peak located at 433 nm, which is the T_1 to T_n transition of anthracene. There were no transient signals corresponding to singlet states of these ligands, nor their radical cations or anions. Fig. 3a shows the TA spectra of CdSe/**9-ADTC** changing with time as an example. The TA spectra for the other five CdSe/ transmitter complexes are in Fig. S3.

Transient kinetics of the ground state recovery of CdSe NC reveals the rate of TET from CdSe NCs is higher for the **9-ACA** transmitter compared to the 1- and 2- isomers. Kinetics were monitored around the first exciton absorption, reflecting the generation of anthracene triplets. An empirical stretching exponential (eq. 2) was used to model the dynamics of interfacial TET and the ground state recovery of CdSe NCs (eq. 2 to 4) and fitting values are listed in Table S2.[13]

$$\Delta A = A \cdot exp(-\left(\frac{t}{\tau}\right)^{\beta}) \quad \text{(eq. 2)}$$

Where A and τ are the amplitude and the stretched lifetime respectively, corresponding to the TET between CdSe and the surface-bound acceptor. β is the stretching exponent. Using

$$< \tau >= \frac{\tau}{\beta} \cdot \Gamma(\frac{1}{\beta}) \quad \text{(eq. 3)}$$

The average weighted lifetime, $<\tau>$, was calculated using τ and β.

$$< k >= \frac{1}{<\tau>} - \frac{1}{<\tau_0>} \quad \text{(eq. 4)}$$

As shown in equation 3 and Table 1, we calculate the average rate of energy transfer, $<k>$, with parameters from the fits, showing that CdSe/9-isomers have the highest energy transfer rate, an order of magnitude higher than CdSe/1- and CdSe/2-isomers. For example, $<k_{9\text{-}ACA}>$ and $<k_{9\text{-}ADTC}>$ are 3.8×10^7 and 2.7×10^7 s^{-1} respectively, while the corresponding rate for the other isomers range from 2.7×10^5 to 6.5×10^5 s^{-1}. This makes sense for **9-ACA** because this transmitter always gives an upconversion QY exceeding 10%, while the upconversion QY for the 1- and 2- transmitters is between 1-3%. The measured $<k_{9\text{-}ACA}>$, 3.8×10^7 s^{-1} (Table 1), is in agreement with the value reported by Bardeen,[11] 1.5×10^7 s^{-1}, obtained from time resolved photoluminescence spectroscopy (TRPL), and also in agreement with Li et al's 1.0×10^7 s^{-1} rate.[10] However, $<k_{9\text{-}ACA}>$ here is two orders of magnitude lower than the 3×10^9 s^{-1} from Castellano's work[13], perhaps because they treated their CdSe/ **ODPA** NCs with oleic acid before ligand exchange, resulting in an average of 12 ligands per CdSe NC, N =3 for CdSe/**9-ACA** here.

We hypothesize that the discrepancy between the fast recovery of the exciton bleach for the CdSe/ **9-ADTC** NCs, $<k_{9\text{-}ADTC}>$, and its low upconversion QY is related to the fast quenching of the excited state. This is reflected in the low fluorescence QY of **9-ADTC** (0.05%), which indicates intersystem crossing (ISC), internal conversion and other nonradiative decay pathways such as the nπ* transitions from the lone pair on the nitrogen atom of the **DTC** group to the anti-bonding orbital on the anthracene ring are dominant. The fluorescence QY of six isomers in THF under N_2 atmosphere at RT are shown in Fig. 4a and Table S2. We found that the **ACA** isomers have a much higher fluorescence QY (0.2 - 0.4), compared to 0.0005 - 0.012 of the **ADTC** isomers. In THF, the 2-isomers have the highest fluorescence QY for both **ACA** and **ADTC** isomers. We also considered hole transfer as a possible reason for the low upconversion QY for the CdSe/**9-ADTC** NCs, especially since Weiss et al recently reported enhanced hole transfer from CdSe NCs to phenothiazine when covalently linked by phenyl dithiocarbamate.[28] To investigate if this process was thermodynamically feasible, we used cyclic voltammetry (CV) to measure the HOMO and LUMO of **9-ACA** and **9-ADTC** (Fig. S4). The molecular orbital levels are depicted in Fig. 4b with the conduction and valance band of CdSe NCs[27]. From the energy diagram, hole transfer from CdSe NCs to bound **ACA** or **ADTC** isomers is possible, though there is not a large thermodynamic driving force.

Conversely, electron transfer from ligands to CdSe QDs is also possible. However, there is no evidence of radical cation or radical anion formation for CdSe/1-, 2- and 9-**ADTC** complexes as there are no changes in the kinetic traces extracted from our TA spectra at 629 nm, 681 nm and 748 nm (anthracene radical cation[29]), or 452 nm, 596 nm and 732 nm (anthracene radical anion[30]). In addition, unlike the Weiss group, we did not observe a red shift in the absorption spectrum of the CdSe NCs after ligand exchange with the **ADTC** isomers, further discounting hole delocalization.

The larger $<k_i>$measured for the 9-isomers implies they are more effective transmitters. The 9-isomers may bind selectively to unique facets on the CdSe NC distinct from that for the 1- and 2- isomers. This might affect the electronic coupling with the NC, critical to efficient Dexter energy transfer across the molecular-nanocrystal interface[10]. The average number of bound ligands per CdSe, N, has a maximum value when functionalized with the 1- or 2- isomers, while N continuously increases with the 9- isomers as a function of transmitter concentration (Fig. S1). This qualitative difference

View Article Online
DOI: 10.1039/C6CC08229G

indicates that molecular geometry might affect binding affinity, especially since anisotropic wurtzite CdSe NCs are employed here. In principle, these NCs have Cd^{2+} and Se^{2-} rich facets on opposing ends of the wurtzite *c*-axis, and Guyot-Sionnest has reported that 2.7 nm wurtzite CdSe/ **ODPA** NCs have a dipole moment of 40 Debye. Anisotropy not-withstanding, zinc blende CdSe NCs also have a permanent dipole, perhaps due to surface charges.[31]

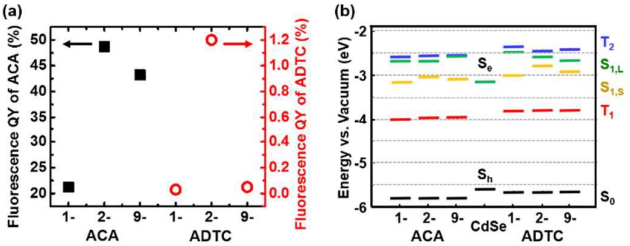

Fig. 4 (a) Fluorescence QY (%)of **ACA** (black square) and **ADTC** (red circle) isomers in anhydrous THF at RT. (b) Band offsets for CdSe NCs (diameter, d = 2.4 nm)[1] The HOMOs of **ACA** and **ADTC** were measured by cyclic voltammetry (CV) in dichloromethane. The first excited singlet state in THF and 4-Bromopolystyrene (4-BrPS) is denoted as $S_{1,\,L}$ and $S_{1,s}$ respectively. The first and second triplet excited state, T_1 and T_2 were measured from isolated anthracene molecules dispersed in 4-BrPS at RT.

The dielectric environment of the anthracene transmitter will affect its excited state energy levels, while its orientation with respect to the NC surface will affect the electronic coupling. For example, in isolated anthracene molecules, the T_2 state is below the S_1 state, resulting in efficient ISC and a low fluorescence QY. However, the relative energy values of these two states are reversed in crystalline anthracene, with T_2 being 73 meV higher in energy than the S_1, thus decreasing the rate of ISC.[32] In another example, for the single perylene diimide (PDI) molecule, the yield of triplets is less than 1%, but a cofacially stacked PDI-dimer forms an excimer with up to 50% yield of triplets from the initial excitations.[33] While it would be ideal to characterize the tilt angle or symmetry in the binding of the anthracene transmitter ligand to the NC surface, it is experimentally challenging to do so- the use of infrared spectroscopy to measure binding modes was inconclusive. Instead, we have measured the first and second triplet excited state levels (T_1 and T_2 respectively) of isolated anthracene transmitters embedded in 4-bromopolystyrene (4-BrPS).[34] As shown in Fig. 4b, the T_1 to S_0 states cluster around 1.83 eV, while the T_2 to T_1 states are around 1.40 eV, in line with excited states of anthracene in poly (methyl methacrylate).[35] values are shown in Table S3. However, the fluorescence of these isomers in THF or in 4-BrPS show no trend, indicating that the dielectric environment must greatly affect the planarity of the entire molecule and its radiative decay.

The kinetic traces from the TA data shows that the 9-isomers, regardless of functional group, have the highest rate of TET or charge transfer from CdSe NCs to anthracene. TA experiments confirm that the 1-isomers have a higher rate of TET compared to the 2-isomers, which is reflected in the 3% photon upconversion QYs for the former compared to 1% for the latter. Though the **DTC** functional group has a higher binding affinity for the CdSe donors, the **9-ACA** transmitter outperforms the **9-ADTC** by more than two orders of magnitude in terms of photon upconversion. While prior work suggests the poor performance of **9-ADTC** is due to charge transfer to sulphur containing ligands from the NC, it could also stem from the fast non-radiative processes inherent in the **DTC** family that quench molecular excited states particularly when the acid group is in the 9-position. This study shows that molecular orientation greatly affects TET, most likely by affecting orbital overlap between the NC donor and anthracene acceptor. It confirms that small perturbations to molecular structure can drastically realign the relative levels of excited states, thus impacting TET transfer in this hybrid platform.

MLT acknowledges ARO W911NF-16-1-0523 for instrumentation and NSF CHE-1351663 for supplies. VIV and JJR acknowledge NSF CHE 1465284. We thank Prof. Juchen Guo and Linxiao Geng for their help with cyclic voltammetry.

Notes and references

1 J. H. Olshansky, T. X. Ding, Y. V. Lee, S. R. Leone and A. P. Alivisatos, *J. Am. Chem. Soc.*, 2015, **137**, 15567.
2 G. Xing, N. Mathews, S. Sun, S. S. Lim, Y. M. Lam, M. Grätzel, S. Mhaisalkar and T. C. Sum, *Science*, 2013, **342**, 344.
3 S. D. Stranks, G. E. Eperon, G. Grancini, C. Menelaou, M. J. Alcocer, T. Leijtens, L. M. Herz, A. Petrozza and H. J. Snaith, *Science*, 2013, **342**, 341.
4 J. H. Heo, H. J. Han, D. Kim, T. K. Ahn and S. H. Im, *Energy Environ. Sci.*, 2015, **8**, 1602.
5 J. Burschka, N. Pellet, S.-J. Moon, R. Humphry-Baker, P. Gao, M. K. Nazeeruddin and M. Grätzel, *Nature*, 2013, **499**, 316.
6 B. O'regan and M. Grätzel, *Nature*, 1991, **335**, 737.
7 L. Kavan, M. Grätzel, S. Gilbert, C. Klemenz and H. Scheel, *J. Am. Chem. Soc.*, 1996, **118**, 6716.
8 M. Grätzel, *Nature*, 2001, **414**, 338.
9 Z. Huang, X. Li, M. Mahboub, K. M. Hanson, V. M. Nichols, H. Le, M. L. Tang and C. J. Bardeen, *Nano Lett.*, 2015, **15**, 5552.
10 X. Li, Z. Y. Huang, R. Zavala and M. L. Tang, *J. Phys. Chem. Lett.*, 2016, **7**, 1955.
11 G. B. Piland, Z. Huang, M. Lee Tang and C. J. Bardeen, *J. Phys. Chem. C*, 2016, **120**, 5883.
12 M. Mahboub, H. Maghsoudiganjeh, A. M. Pham, Z. Huang and M. L. Tang, *Adv. Funct. Mater.*, 2016, **26**, 6091.
13 C. Mongin, S. Garakyaraghi, N. Razgoniaeva, M. Zamkov and F. N. Castellano, *Science*, 2016, **351**, 369.
14 M. Wu, D. N. Congreve, M. W. Wilson, J. Jean, N. Geva, M. Welborn, T. Van Voorhis, V. Bulović, M. G. Bawendi and M. A. Baldo, *Nat. Photon.*, 2016, **10**, 31.
15 A. Hagfeldt, G. Boschloo, L. Sun, L. Kloo and H. Pettersson, *Chem. Rev.*, 2010, **110**, 6595.
16 M. Grätzel, *J. Photochem. Photobiol., C*, 2003, **4**, 145.
17 P. Qin, X. Yang, R. Chen, L. Sun, T. Marinado, T. Edvinsson, G. Boschloo and A. Hagfeldt, *J. Phys. Chem. C*, 2007, **111**, 1853.
18 N. Koumura, Z.-S. Wang, S. Mori, M. Miyashita, E. Suzuki and K. Hara, *J. Am. Chem. Soc.*, 2006, **128**, 14256.
19 A. Kearvell and F. Wilkinson, *Molecular Crystals*, 1968, **4**, 69.
20 A. Kearvell and F. Wilkinson, *J. Chim. Phys.(Paris, 1969)*, 1969, 125.
21 N. J. Turro, V. Ramamurthy and J. C. Scaiano, *Modern molecular photochemistry of organic molecules*, University Science Books Sausalito, California, 2010.
22 T. C. Werner and D. M. Hercules, *J. Phys. Chem.*, 1969, **73**, 2005.
23 N. Ghoneim, D. Scherrer and P. Suppan, *J. Lumin.*, 1993, **55**, 271.
24 C. Hong, W. Luo, D. Yao, Y. Su, X. Zhang, R. Tian and C. Wang, *Biorg. Med. Chem.*, 2014, **22**, 3213.
25 J. Zhu, L. Han, Y. Diao, X. Ren, M. Xu, L. Xu, S. Li, Q. Li, D. Dong and J. Huang, *J. Med. Chem.*, 2015, **58**, 1123.
26 C. Jia and X. Guo, *Chem. Soc. Rev.*, 2013, **42**, 5642.
27 M. T. Frederick, V. A. Amin, N. K. Swenson, A. Y. Ho and E. A. Weiss, *Nano Lett.*, 2013, **13**, 287.
28 S. Lian, D. J. Weinberg, R. D. Harris, M. S. Kodaimati and E. A. Weiss, *ACS Nano*, 2016, **10**, 6372.
29 J. Masnovi, E. Seddon and J. Kochi, *Can. J. Chem.*, 1984, **62**, 2552.
30 S. U. Pedersen, T. B. Christensen, T. Thomasen and K. Daasbjerg, *J. Electroanal. Chem.*, 1998, **454**, 123.
31 M. Shim and P. Guyot-Sionnest, *J. Chem. Phys.*, 1999, **111**, 6955.
32 W. T. Stacy and C. E. Swenberg, *J. Chem. Phys.*, 1970, **52**, 1962.
33 T. A. Ford, I. Avilov, D. Beljonne and N. C. Greenham, *Phys. Rev. B*, 2005, **71**, 125212.

View Article Online
DOI: 10.1039/C6CC08229G

34 S. Reineke and M. A. Baldo, *Sci Rep*, 2014, **4**, 3797.
35 M. R. Padhye, S. P. McGlynn and M. Kasha, *J. Chem. Phys.*, 1956, **24**, 588.